Available online at www.sciencedirect.com

ScienceDirect

Procedia Structural Integrity 13 (2018) 149–154

Structural Integrity Procedia

www.elsevier.com/locate/procedia

ECF22 - Loading and Environmental effects on Structural Integrity

Tensile and compression properties of variously arranged porous Ti-6Al-4V additively manufactured structures via SLM

S.Raghavendra[a]*, A.Molinari[a], V.Fontanari[a], V.Luchin[b], G.Zappini[b], M.Benedetti[a], F.Johansson[c], J.Klarin[c]

[a]*Department of Industrial Engineering,University of Trento,Trento 38123,Italy*
[b]*Eurocoating Spa, Pergine Valsugana, Trento 38057, Italy*
[c]*Product Development and Materials Engineering,Jönköping University, Jönköping 55318, Sweden*

Abstract

Additively manufactured porous structures find increasing applications in the biomedical context to produce orthopedic prosthesis and devices. In comparison with traditional bulk metallic implants, they permit to tailor the stiffness of the prosthesis to that of the surrounding bony tissues, thus limiting the onset of stress shielding and resulting implant loosening, and to favor the bone in-growth through the interconnected pores. Mechanical and biological properties of these structures are strongly influenced by the size and spatial arrangement of pores and struts. In the present work irregular and regular cellular as well as fully random porous structures are investigated through tensile and compression uniaxial tests. Specific point of novelty of this work is that, beside classical compressive tests, which are standard characterization methods for porous/ cellular materials, tensile tests are carried out. Mechanical tests are complemented with morphological analysis and porosity measurements. An attempt is made to find correlations between cell arrangements, porosity and mechanical properties.

Peer-review under responsibility of the ECF22 organizers.

Keywords: Cellular structures; porosity; Strength

1. Introduction

Titanium alloys are the most preferred materials for production of bio-implants, as they exhibit high strength-to-weight ratio, good corrosion resistance and excellent biocompatibility. However, there is still a mismatch in the elastic modulus of titanium implants and bone tissues surrounding the implant, which leads to stress shielding in that region.

* Corresponding author. Tel.: +39-348-381-7779; fax: +0-000-000-0000 .
E-mail address: sunil.raghavendra@unitn.it

2452-3216
Peer-review under responsibility of the ECF22 organizers.
10.1016/j.prostr.2018.12.025

To reduce the mismatch in these properties, solid implants are being replaced by cellular or porous structures (Cheng et al., 2012; Garrett et al., 2006). It is observed that cellular structures can assist in development of tissues inside the implants (also called "bone in-growth"). Cellular structures beneficially reduce the stress shielding phenomenon, but they also decrease the fatigue resistance of the implants (Taniguchi et al., 2016). Additive manufacturing (AM) employs layer-wise material addition technique to build such structures. Selective laser melting (SLM) and Electron beam melting (EBM) are the most widely used AM techniques for titanium alloys. SLM technique is often preferred because of its higher ability to control the geometrical properties of the structures. (Dallago et al., 2018).

In general, studies indicate that higher porosity level leads to lower strength and stiffness, but for certain geometries, for example the octet basic cell, the decrease in strength ends for a porosity of 75% (Arabnejad et al., 2016). Several studies have also indicated that cell topology and microstructure also affect the mechanical properties in different ways. There are studies on compression and tensile testing of trabecular structures which show that the tensile strength is slightly lower than the compressive strength (Maskery et al.,2015). The major challenge in the field of porous cellular or porous trabecular structures is to understand the effect of different geometrical parameters on the strength and stiffness of the trabecular structure.

In this current work we aim at understanding the effect of different type of cellular structures and porosity values on mechanical properties. Morphological analysis is carried out to obtain the unit cell properties such as strut thickness and void size to understand the geometrical deviation in the manufactured structures. To understand the mechanical properties of trabecular structures, both monotonic and cyclic compression and tension tests are carried out.

2. Materials and methods

In this section, a description about the material used and the design of specimen is given. Methods used in the experimental investigation, which include surface and mechanical characterization, are discussed.

2.1. Specimen design

The material used in this research project was the Titanium alloy Ti-6Al-4V, also called Ti64, which is one of the most widely used biomedical alloys. Different specimen geometries with specific characteristics have been investigated. Three different batches of specimens (A, B and C) were manufactured with three different cellular structures namely irregular, regular and fully random cellular structure in each batch as shown in Fig.1 for batch A. Table 1. gives a detailed explanation of specimen parameters. The combination of large struts and small voids was not considered since it would result in non-interconnected pores, which would not support the bone in-growth. All the specimens were subjected to heat treatment process to eliminate the residual stresses from the SLM process and prevent their effect on the results.

Table 1. Void size and strut thickness of different batches (nominal values, from CAD files)

Batch	Void Size (μm)	Strut thickness(μm)
A	1500	500
B	700	200
C	1500	200

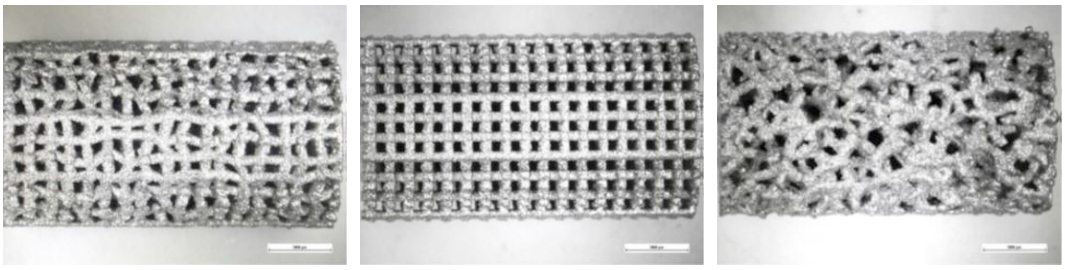

Fig. 1. Lateral view of Batch A Samples: (a) Irregular structure (b) Regular structure (c) Fully random structure

2.2. Experimental

The morphological, metallographic and mechanical properties were analyzed to obtain a complete characterization of the specimens. This section discusses the experimental methods used in the current investigation.

Porosity fraction of the specimens was determined using the relative density of the specimen and the theoretical density of 4.42 g/cm3 for Ti-6Al-4V alloy, by using equation 1 where ρth is the theoretical density, mass and volume are calculated for each specimen (Mullen et al., 2009).

$$Porosity = \frac{\rho th - \left(\frac{mass}{volume}\right)}{\rho th} \quad (1)$$

Before measuring the mass, the specimens were cleaned with ethanol, subjected to ultrasound for 5 minutes and then dried in a furnace at 120°C for 2 hours to remove loose particles from the manufacturing process. The mass was determined by means of an analytical balance having a precision of 0.0001 mg. The volume was measured by a digital caliper taking measurements in different positions.

To perform morphological characterization, the specimens were analyzed by Nikon stereomicroscope and JEOL JSM-IT300LV scanning electron microscope (SEM). Horizontal and lateral surfaces of the specimen were investigated for strut thickness, void size and to observe the shape of the strut. (Sympatec GmBH, 2017; Kasperovich et al.,2015).

The compression and tensile test were carried out under two conditions, viz. quasi-static and cyclic. Instron 8516 testing machine was used for both compression and tensile test. The tests were performed and elastic modulus was calculated according to ISO standard 13314:2011 for compression and tensile test (Dallago et al., 2018, 2011; ISO Standard,2011). Total of 3 samples for quasi-static and 2 samples for cyclic tests were considered for each structure. The compression test specimens initially had a height-to-diameter ratio of 2:1, as suggested by ISO 13314. To avoid the tendency of buckling that was observed during preliminary testing, the height-to-diameter ratio in specimens was reduced to 1:1, Fig.2a-2b. The tensile test specimen consisted of cellular structure between two solid threaded pieces, Fig. 2c, the connection between the cellular region and thread was made stiffer to avoid failure at the junction.

Quasi-static tests were carried out under displacement control at a rate of 2mm/min and data sampling frequency of 1 kHz. The strain was recorded using a LVDT (Linear Variable Displacement Transducer) for compression test and a 12.5mm extensometer for tensile test. The Young's modulus in compression and tension was calculated in the 20-70% of yield strength region for both quasi static and cyclic tests. In compression test, offset yield strength was found by creating an offset line at 0.2% parallel to the slope of Young's Modulus. Maximum strength (offset compressive strength) was found by a parallel offset line at 4% from yield strength line. In tensile test, yield strength and ultimate tensile strength was obtained from the stress-strain curve.

Cyclic tests were conducted under load control with a triangular wave shape comprised between 20% and 70% of plateau stress for compression tests and 20% and 70% of elastic limit for tensile tests (Dieter,1988; Gross 2014; Abbaschian,1994) until cycle stabilization which occurred within 5 cycles.

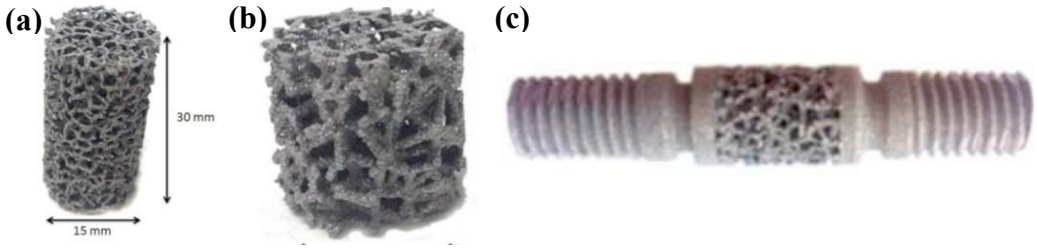

Figure 2 (a) Compression test specimen with l/d ratio 2 (b) Compression test specimen with l/d ratio 1 (c) Tensile test specimen

3. Results and discussion

3.1. Porosity

Highest porosity was observed for batch C followed by batch A and batch B. The difference between the real porosity and designed porosity is shown in table 2. A maximum deviation in geometry of 45.4% was observed for batch B, while for batch A and batch C the deviation was 16.4%.

Table 2. Comparison of measured and designed porosity

Sample	Batch A Measured (%)	Batch A Designed (%)	Batch B Measured (%)	Batch B Designed (%)	Batch C Measured (%)	Batch C Designed (%)
Irregular	57.1(0.7)	75.4	38.9(0.3)	78.5	75.6(0.2)	92.9
Regular	59.6(0.8)	75.6	44.3(0.5)	80.0	77.3(0.1)	93.2
Fully Random	58.6(0.3)	63.3	45.5(0.6)	71.9	76.3(0.2)	92.4

3.2. Morphological analysis

The results indicate that the specimens of batch A and batch C had larger void compared to batch B. Batch B and C had thinner struts while batch A consisted of thicker struts. These facts are consistent with the designed values, but the measured dimensions indicated an increase of the struts thickness of approximately 200µm and correspondingly a decrease of the void size. The reason for such increase is related to the presence of partially melted particles on the strut surfaces, the dimensions of the melt pool and the laser scan parameters. The deviation in thickness values was larger along the direction perpendicular to the build plate than on directions parallel to the build plate. This difference between designed and actual dimensions influenced the change in porosity seen in section 3.1.

3.3. Compression and tensile test

The effect of porosity on the strength and stiffness of the structure is as shown in fig.3, and 4 respectively. The results indicated that strength and stiffness of the material decrease with increase in porosity. The ultimate tensile strength of the material is lower than offset compressive strength by an average value of 100MPa in all the structures of batch A and batch B, while it is marginally lower in batch C as shown also in Fig. 6a.

Young's modulus from both quasi-static and cyclic tensile test ranges between 16–20 GPa, 43–47 GPa and 7–13 GPa in batches A, B and C respectively, while in quasi-static and cyclic compression it ranges between 7–12 GPa, 9–16 GPa and 1–3 GPa in batches A, B, C, respectively. The structures of batch B reached the highest values of tensile and compressive strength, followed by batch A and batch C specimens as shown in Fig.3b, 4b and 5b respectively. The value of the Young's modulus in cyclic tests stabilized from the 2nd loading cycle as shown in Fig.5a.

The results also suggest that, with similar values of actual porosity, the regular structures possess the highest values of stiffness and strength, while random structures show the lowest values. This is especially valid for the specimens of batch A and C: for example, with a real porosity of 57-59%, the average compressive strength is 210 MPa for a regular, 198 MPa for irregular and 170 MPa for random structure. Similarly, the compressive Young's modulus decreases from 11.9 GPa, to 9.2 GPa, to 6.8 GPa. Similar conclusions can be drawn for ultimate tensile strength and tensile modulus.

The comparison between tensile and compression data is represented in Fig. 5a, 5b and 6b. These cellular structures possess higher compressive strength than tensile strength, yet the differences are lower with increasing porosity. The compressive modulus, on the other hand, is much smaller than the tensile modulus for all kinds of specimens.

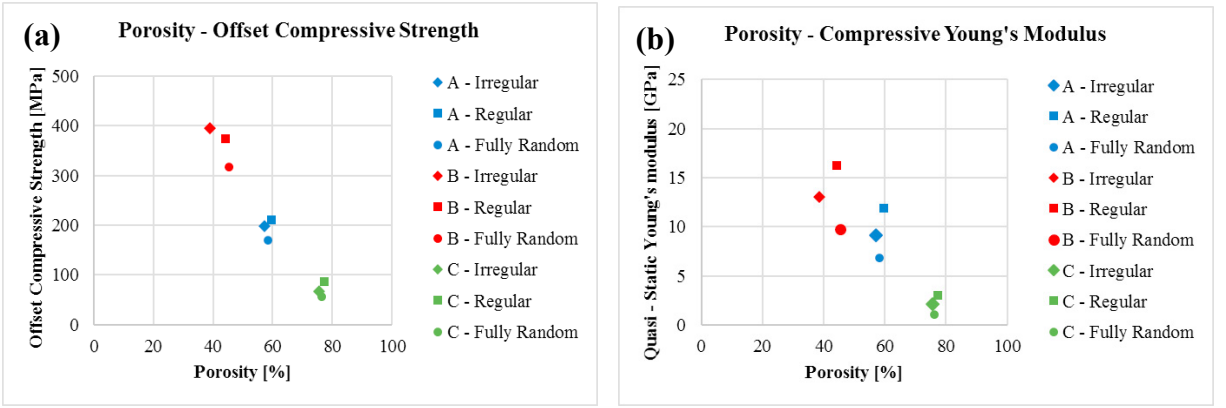

Fig. 3 Compression test for different porosity (a) Offset compressive strength (b) Quasi – Static Young's modulus

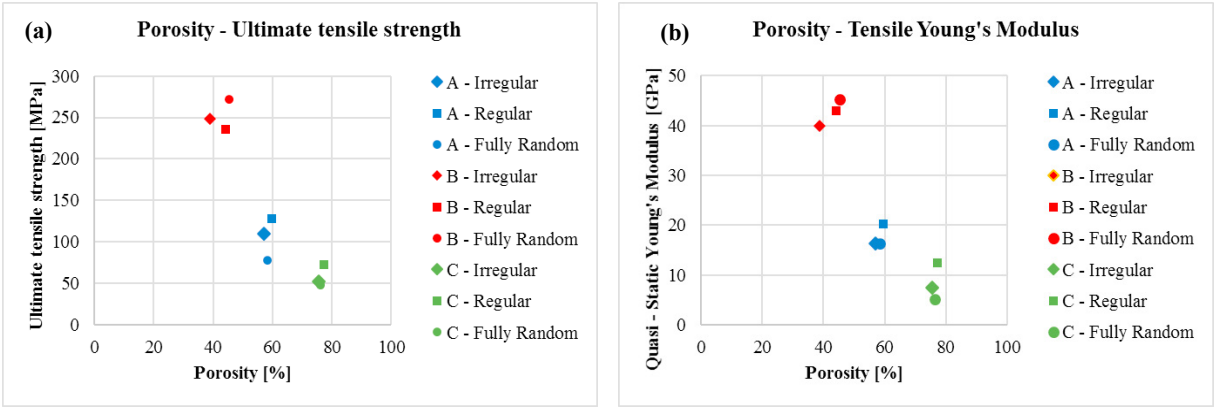

Fig. 4 Tensile test for different porosity (a) Ultimate Tensile Strength (b) Quasi - Static Young's modulus

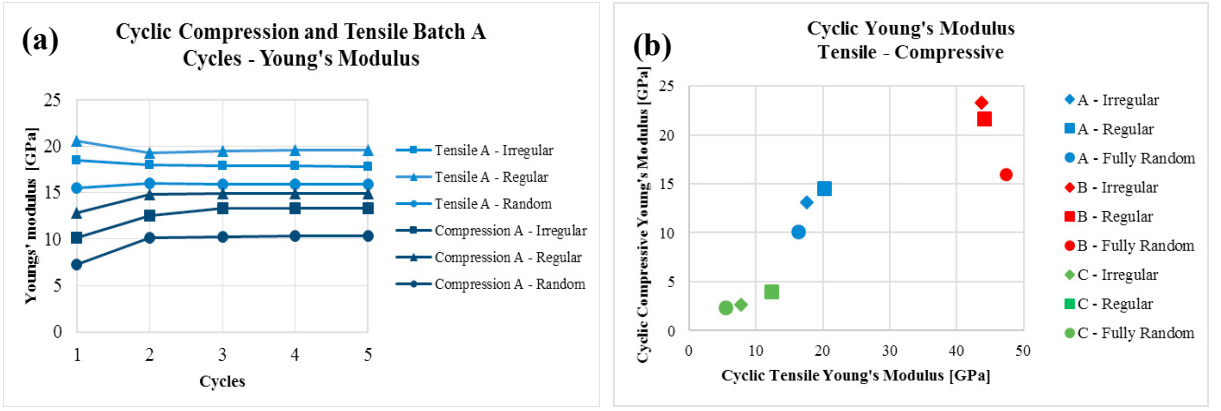

Fig. 5 Cyclic Test (a) Batch A Cyclic Tensile and Compression Test (b) Cyclic Young's Modulus

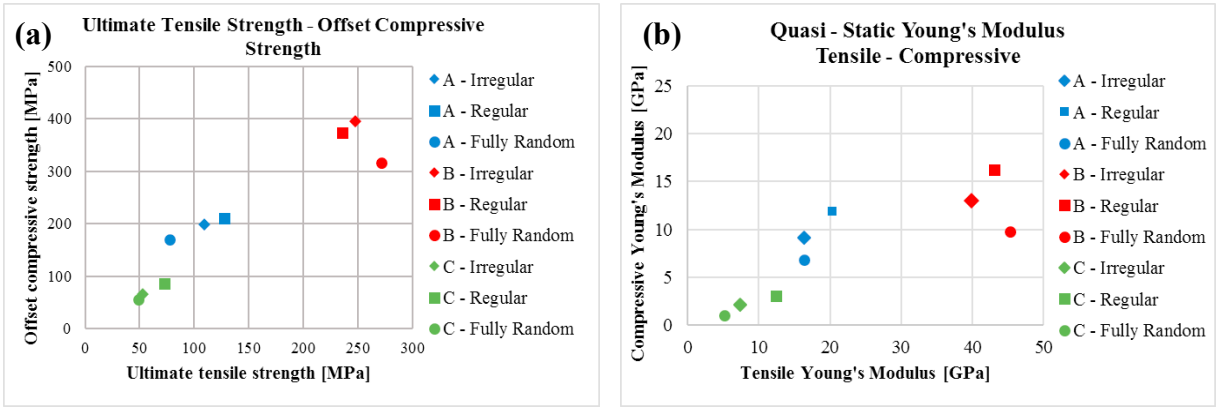

Fig. 6 (a) Strength in Compression and Tensile (b) Quasi – Static Young's modulus in compression and tensile

The orientation of the structures plays also a role in the determination of its properties: the reason for the better behavior of regular structures is related to the fact that many struts are aligned with the direction of the compressive/tensile force. A different orientation of the structure might lead to different outcomes. Theoretically, the more random the structure, the less the influence of its orientation related to the direction of the external force. This aspect will be addressed in a future work.

4. Conclusion

The results of the study include dimensional and mechanical characterization of irregular, regular and fully random cellular structures with different cell characteristics. Compression and tensile tests were carried out to analyse their mechanical properties. The conclusions drawn from the study are as follows.

- The results indicated a decrease in the actual porosity compared to the designed values. In order to obtain the desired porosity, the designed structures should have higher porosity fraction than the required porosity.
- During preliminary compression tests, a clear tendency of buckling was observed, which is usually seen in specimens with high porosity. A reduction of the height-to-diameter ratio from 2:1 to 1:1 is needed for such structures in order to induce deformation by yielding.
- The strength and Young's modulus decrease considerably with increasing porosity for quasi-static and cyclic compression and tensile test. The tensile strength of the structures was marginally lower when compared to compression test, while Young's modulus was significantly higher in tensile compared to compression test values.
- The regular structures showed marginal differences compared to their respective deformed irregular structures. Especially with high values of porosity, regular structures showed slightly higher mean values of strength and stiffness. Fully random structures possessed slightly lower values. This indicates that porosity values still play a major role compared to the type of structure.
- This conclusion is related to one single orientation of the structures in relation to the external force. The study shall be completed and its outcome confirmed by analysing the influence of the orientation angle.

Acknowledgements

This work is part of the FAMAC Research Project, co-sponsored by Eurocoating S.p.A. and Provincia Autonoma di Trento (Regional Public Authority).

References

Cheng, X Y., Li, S J., Murr L E., Zhang, Z B., Hao, Y L., Yang, R., Medina, F., Wicker, R B., 2012. Compression Deformation Behavior of Ti–6Al–4V Alloy with Cellular Structures Fabricated by Electron Beam Melting. J. of the Mechanical Behavior of Biomedical Materials 16,153 – 162.

Garrett, R., Abhay, P., Dimitrios Panagiotis, A., 2006. Fabrication Methods of Porous Metals for use in Orthopedic Applications. Biomaterials 27, 2651-2670.

Naoya Taniguchi, Shunsuke Fujibayashi, Mitsuru Takemoto, Kiyoyuki Sasaki, Bungo Otsuki, Takashi Nakamura, Tomiharu Matsushita, Tadashi Kokubo, Shuichi Matsuda, 2016. Effect of Pore Size on Bone Ingrowth into Porous Titanium Implants Fabricated by Additive Manufacturing: An In Vivo Experiment. Materials Science and Engineering C 59, 690–701.

Dallago, M., Fontanari, V., Torresani, E., Leoni, M., Pederzolli, C., Potrich, C., Benedetti, M., 2018. Fatigue and Biological Properties of Ti-6Al-4V ELI Cellular Structures with Variously Arranged Cubic Cells Made by Selective Laser Melting. Journal of the Mechanical Behavior of Biomedical Materials 78, 381-394.

Arabnejad, S., Burnett Johnston, R., Pura, J A., Singh, B., Tanzer, M., Pasini, D., 2016. High Strength Porous Biomaterials for Bone Replacement: A Strategy to Assess the Interplay Between Cell Morphology, Mechanical properties, Bone ingrowth and Manufacturing constraints. Acta Biomaterialia 30, 345-356.

F. Dimaano, F., Hermida, J., D'Lima, D., Cowell, C., Kulesha, G., 2010. Comparison of the Coefficient of Friction of Porous Ingrowth Surfaces. 56th Annual Meeting of the Orthopedic Research Society. La Jolla.

Maskery, I., Aremu, A O., Simonelli, M., Tuck, C., Wildman, R D., Ashcroft, I A., Hague, R J., 2015. Mechanical Properties of Ti-6Al-4V Selectively Laser Melted Parts with Body-Centered-Cubic Lattices of Varying cell size. Experimental Mechanics 55, 1261-1272.

Mullen, L., Stamp, R C., Fox, P., Jones, E., Ngo, C., Sutcliffe, C J., 2010. Selective Laser Melting: A Unit Cell Approach for the Manufacture of Porous, Titanium, Bone In-Growth Constructs, Suitable for Orthopedic Applications. II. Randomized Structures. Journal of Biomedical Research Materials, Part B Applied Biomaterials 92,178-188.

Kasperovich, G., and Hausmann, J., 2015. Improvement of Fatigue Resistance and Ductility of Ti-6Al-4V Processed by Selective Laser Melting. Journal of Material Processing Technology 220, 202-214.

Sympatec GmbH, May 2017. Particle Characterisation. www.sympatec.com/en/particle-measurement/glossary/particle-shape.

ISO Standard, ISO 13314, 2011. Mechanical testing of metals – Ductility testing – Compression test for porous and cellular metals. International Organization of Standards, Switzerland. www.iso.org

Dieter, G E., 1988. Mechanical Metallurgy (third edition), McGraw-Hill. New York, USA.

Abbaschian, R., Abbaschian, L., Reed-Hill, R E., 1994. Physical Metallurgy Principles (fourth edition), Cengage Learning. Stamford, USA.

Gross, D., Hauger, W., Schröder, J., Wall, W A., Govindjee, S., 2014. Engineering Mechanics 3 - Dynamics (second edition), Springer, Berlin, Germany.